Finite-Element Analysis of Dielectric-Loaded Waveguides

MITSUO HANO

Abstract—**A finite-element analysis in which nonphysical spurious solutions do not appear has been established to solve the electromagnetic field problem of the closed waveguide filled with various anisotropic media. This method is based on the approximate extremization of a functional, whose Euler equation is the three-component curlcurl equation derived from the Maxwell equations, with a new conforming element. Specific examples are given and the results are compared with those obtained by exact solutions and longitudinal two-component finite-element solutions. Very close agreement was found and all nonzero eigenvalues have been proved to have one-to-one correspondence to the propagating modes of the waveguide.**

I. Introduction

As a result of the broad variety of practical applications of the closed waveguide filled with several kinds of media in microwave and optical frequency regions, the development of methods to solve the associated electromagnetic field problems has attracted the attention of many researchers. The finite-element method, which enables one to compute accurately the mode spectrum of a waveguide with arbitrary cross section, has been widely used [1]–[7]. However, the two-component finite-element solutions have been known to include nonphysical spurious modes [2], [3].

Konrad has derived a three-component vector variational expression for electromagnetic field problems [5], and has selected a family of functions, as a trial solution, in which each component of the vector field is continuous along all interelement boundaries [6]. Therefore, the material parameters are restricted; either permittivity or permeability should be constant in all regions. Spurious solutions have likewise appeared as the result of this numerical calculation.

We investigated his three-component formulation for the condition required of trial solutions, and have concluded that the necessary and sufficient requirement for the trial solution is not so strict as the one in [6].

In this paper, the functional describing the behavior of the electromagnetic fields in anisotropic waveguides is introduced and the set of trial functions perfectly satisfying the boundary conditions required in the functional, a so-called conforming element, is derived. This approach has improved the following two serious problems which are inevitable in the previous two-component and three-component finite-element methods:

1) occurrence of the nonphysical spurious solution,
2) restriction on the discontinuity of either permittivity or permeability of the media.

Manuscript received February 14, 1983; revised May 21, 1984.

The author is with the Department of Electrical Engineering, Yamaguchi University, Tokiwadai, Ube 755, Japan.

II. Variational Formulation of the Maxwell Equations

Consider an arbitrarily shaped metal waveguide immersed in several anisotropic and lossless dielectrics as shown in Fig. 1. This waveguide is assumed to be uniform along its longitudinal z axis. $\hat{\epsilon}$ and $\hat{\mu}$ denote the tensor permittivity and the tensor permeability without off-diagonal elements, respectively, and they are assumed to be constant in each region.

Maxwell curl equations for time-harmonic fields are

$$\nabla \times \boldsymbol{H} = j\omega\hat{\epsilon}\boldsymbol{E} \tag{1}$$

$$\nabla \times \boldsymbol{E} = -j\omega\hat{\mu}\boldsymbol{H} \tag{2}$$

where the vectors $\boldsymbol{E}$ and $\boldsymbol{H}$ are the dielectric- and the magnetic-field intensity, respectively, and ω is an angular frequency. From (1) and (2), we construct

$$\boldsymbol{E} = -(j/\omega)\hat{\epsilon}^{-1}\nabla \times \boldsymbol{H} \tag{3}$$

$$\boldsymbol{H} = (j/\omega)\hat{\mu}^{-1}\nabla \times \boldsymbol{E}. \tag{4}$$

By taking the curl of (3) and (4), and then substituting into (1) and (2), the following common curlcurl equation is obtained:

$$\nabla \times \hat{p}^{-1}(\nabla \times \boldsymbol{V}) - \omega^2\hat{q}\boldsymbol{V} = 0 \tag{5}$$

where $\boldsymbol{V}$ denotes either $\boldsymbol{E}$ or $\boldsymbol{H}$, and $\hat{p}$ and $\hat{q}$ are the material tensors as shown in Table I.

At the interface of the region, an appropriate boundary condition must be satisfied by the field vectors. The interface continuity between two contiguous media (say the rth and sth) requires that

$$\boldsymbol{n} \times (\boldsymbol{V}^r - \boldsymbol{V}^s) = 0 \tag{6}$$

$$(j/\omega)\boldsymbol{n} \times (\hat{p}_r^{-1}\nabla \times \boldsymbol{V}^r - \hat{p}_s^{-1}\nabla \times \boldsymbol{V}^s) = 0 \tag{7}$$

along their common boundary, where $\boldsymbol{n}$ is a surface normal unit vector. On the other hand, for the electric wall and the magnetic wall, the boundary condition of the electromagnetic field requires either

$$\boldsymbol{n} \times \boldsymbol{V} = 0 \tag{8}$$

0018-9480/84/1000-1275$01.00 ©1984 IEEE

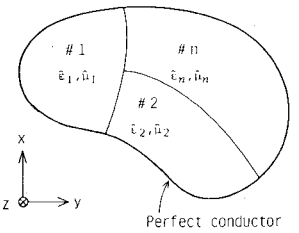

Fig. 1. Configuration of the metal waveguide.

TABLE I
RELATIONS BETWEEN $(\hat{p}, \hat{q})$ AND MATERIAL TENSORS AGAINST V.

V	$\hat{p}$	$\hat{q}$
E	$\hat{\mu}$	$\hat{\epsilon}$
H	$\hat{\epsilon}$	$\hat{\mu}$

or

$$(j/\omega)\boldsymbol{n}\times(\hat{p}^{-1}\nabla\times\boldsymbol{V})=0. \tag{9}$$

The electromagnetic problem defined by (5) with the forced boundary conditions of (6) and (8), is expressed by

$$\delta F=0 \tag{10}$$

in which F is the functional whose variation yields (5) as a Euler equation and (7) and (9) as natural boundary conditions. The functional F is determined to have the form

$$F=\frac{1}{2}\int\{(\nabla\times\boldsymbol{V}^*)\cdot\hat{p}^{-1}(\nabla\times\boldsymbol{V})-\omega^2\boldsymbol{V}^*\cdot\hat{q}\boldsymbol{V}\}\,dv \tag{11}$$

where the asterisk denotes the complex conjugate.

In this paper, traveling waves of the form

$$\boldsymbol{V}=(\boldsymbol{i}_xV_x+\boldsymbol{i}_yV_y+\boldsymbol{i}_zV_z)e^{-j\beta z} \tag{12}$$

are treated, where β is the propagation constant. By substituting (12) into (11), the particular functional is given by

$$\begin{aligned}F=\frac{1}{2}\int\Bigg\{&p_{xx}^{-1}\left|\frac{\partial V_z}{\partial y}\right|^2+p_{yy}^{-1}\left|\frac{\partial V_z}{\partial x}\right|^2+p_{zz}^{-1}\left|\frac{\partial V_y}{\partial x}-\frac{\partial V_x}{\partial y}\right|^2\\&+j\beta p_{xx}^{-1}\left(\frac{\partial V_z^*}{\partial y}V_y-\frac{\partial V_z}{\partial y}V_y^*\right)\\&+j\beta p_{yy}^{-1}\left(\frac{\partial V_z^*}{\partial x}V_x-\frac{\partial V_z}{\partial x}V_x^*\right)\\&+\beta^2\left(p_{xx}^{-1}|V_y|^2+p_{yy}^{-1}|V_x|^2\right)\\&-\omega^2\left(q_{xx}|V_x|^2+q_{yy}|V_y|^2+q_{zz}|V_z|^2\right)\Bigg\}\,ds.\end{aligned} \tag{13}$$

The surface integral in (13) is to be evaluated over the cross section of the waveguide.

III. FINITE-ELEMENT METHOD

The selection of a family of trial solutions for the Rayleigh–Ritz technique is facilitated if the cross section of the waveguide is represented by a series of finite elements. If we consider the subdomain as one region, the trial function is sufficient to satisfy the admissibility requirement presented by the previous section.

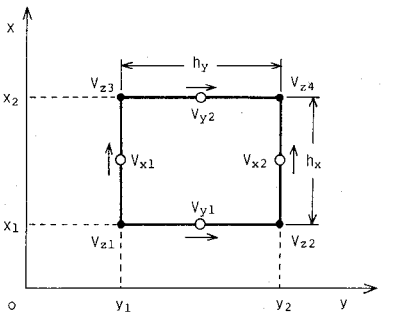

Fig. 2. Rectangular element.

The vector $\boldsymbol{n}\times\boldsymbol{V}$ on the interface of the contiguous regions can be separated into two components: i.e., V_z is a longitudinal component and V_s is a tangential component in the $x-y$ plane. The trial solutions are formed by approximating v_z as a bilinear form of x and y within each element and v_x and v_y as a linear function of x or y. Within each element, the value of v_z is interpolated by the vertex values of V_z, and those of v_x and v_y by the side values of V_x and V_y, respectively, on the element boundary. Fig. 2 illustrates a rectangular element of which side lines are held parallel to the coordinate axes. The eight nodal points described in the element consist of the four corner points (corresponding to unknown values of V_z) and four side points (corresponding to unknown values of V_x and V_y).

Using matrix notation, the approximate vector functional form of $\boldsymbol{v}$ is expressed as

$$\boldsymbol{v}=\{v_x\ v_y\ v_z\} \tag{14}$$

where

$$\left.\begin{aligned}v_x&=\{V_x\}^T[\varphi_x]\\v_y&=\{V_y\}^T[\varphi_y]\\v_z&=\{V_z\}^T[\varphi_z]\end{aligned}\right\} \tag{15}$$

and

$$\left.\begin{aligned}\{V_x\}^T&=\{V_{x1}\ V_{x2}\}\\\{V_y\}^T&=\{V_{y1}\ V_{y2}\}\\\{V_z\}^T&=\{V_{z1}\ V_{z2}\ V_{z3}\ V_{z4}\}\end{aligned}\right\} \tag{16}$$

$$\left.\begin{aligned}[\varphi_x]^T&=[\xi_1\ \xi_2]\\[\varphi_y]^T&=[\zeta_1\ \zeta_2]\\[\varphi_z]^T&=[\zeta_1\xi_1\ \zeta_1\xi_2\ \zeta_2\xi_1\ \zeta_2\xi_2]\end{aligned}\right\} \tag{17}$$

$$\left.\begin{aligned}\zeta_1&=(x_2-x)/h_x, &\zeta_2&=(x-x_1)/h_x\\\xi_1&=(y_2-y)/h_y, &\xi_2&=(y-y_1)/h_y\end{aligned}\right\} \tag{18}$$

and T denotes transverse. Equation (14) can be rewritten as

$$\boldsymbol{v}=\{V\}^T[\Phi] \tag{19}$$

where

$$\{V\}^T = \left(\{V_x\}^T \{V_y\}^T \{V_z\}^T\right) \tag{20}$$

$$[\Phi] = \begin{bmatrix} \varphi_x & 0 & 0 \\ 0 & \varphi_y & 0 \\ 0 & 0 & \varphi_z \end{bmatrix} \tag{21}$$

and [0] is a zero matrix.

The partial derivatives of $[\varphi_x]$, $[\varphi_y]$, and $[\varphi_z]$ of (17) with respect to x and y are given by

$$\left.\begin{aligned} \frac{\partial}{\partial y}[\varphi_x] &= [B_x][\varphi_0], & \frac{\partial}{\partial x}[\varphi_y] &= [A_y][\varphi_0] \\ \frac{\partial}{\partial x}[\varphi_z] &= [A_z][\varphi_x], & \frac{\partial}{\partial y}[\varphi_z] &= [B_z][\varphi_y] \end{aligned}\right\} \tag{22}$$

where

$$\left.\begin{aligned} [B_x] &= \frac{1}{h_y}\begin{bmatrix} -1 \\ 1 \end{bmatrix}, & [A_y] &= \frac{1}{h_x}\begin{bmatrix} -1 \\ 1 \end{bmatrix} \\ [A_z] &= \frac{1}{h_x}\begin{bmatrix} -1 & 0 \\ 0 & -1 \\ 1 & 0 \\ 0 & 1 \end{bmatrix}, & [B_z] &= \frac{1}{h_y}\begin{bmatrix} -1 & 0 \\ 1 & 0 \\ 0 & -1 \\ 0 & 1 \end{bmatrix} \end{aligned}\right\} \tag{23}$$

and

$$[\varphi_0] = [1]. \tag{24}$$

From (22), (23), and (24), the $\nabla \times \boldsymbol{v}$ is derived as follows:

$$\nabla \times \boldsymbol{v} = \{V\}^T [S][\Psi] \tag{25}$$

where

$$[S] = \begin{bmatrix} 0 & -j\beta I & -B_x \\ j\beta I & 0 & A_y \\ B_z & -A_z & 0 \end{bmatrix} \tag{26}$$

$$[\Psi] = \begin{bmatrix} \varphi_y & 0 & 0 \\ 0 & \varphi_x & 0 \\ 0 & 0 & \varphi_0 \end{bmatrix} \tag{27}$$

and $[I]$ is a unit matrix.

On the other hand, from the commutativity of the differential operators $\partial/\partial x$ and $\partial/\partial y$, the following relation is obtained:

$$[B_z][A_y] = [A_z][B_x]. \tag{28}$$

Using the relation of (28), it is derived that the rank of the 8×5 matrix $[S]$ of (26) becomes four. This factor can be explained as follows. From (19) and (25), the curl operator $\nabla \times$ is a linear operator from the space having $[\Phi]$ as a basis to the space having $[\Psi]$ as a basis. Therefore, the operator is a degenerate operator with a kernel, which is the subspace satisfying the following relation:

$$\nabla_t v_z + j\beta \boldsymbol{v}_t = 0 \tag{29}$$

where ∇_t is a transverse operator and $\boldsymbol{v}_t$ is a transverse component of $\boldsymbol{v}$. The nullity of the operator is equal to the dimension of v_z, that is four. The matrix $[S]$ is the matrix representation of the curl operator on the space having $[\Phi]$ as a basis.

Substituting (19) and (25) into (13) and performing the indicated integrations, the contribution of the particular element "e" to the total values of F is obtained. The resulting expression with respect to the parameters gives

$$F^e = \tfrac{1}{2}\left(\{V\}^\dagger [K]\{V\} - \omega^2 \{V\}^\dagger [M]\{V\}\right) \tag{30}$$

in which

$$[K] = [S]^* \left(\iint [\Psi]\hat{p}^{-1}[\Psi]^T dx\,dy\right)[S]^T \equiv \begin{bmatrix} K_{11} & K_{12} & K_{13} \\ K_{21} & K_{22} & K_{23} \\ K_{31} & K_{32} & K_{33} \end{bmatrix} \tag{31}$$

$$[M] = \iint [\Phi]\hat{q}[\Phi]^T dx\,dy \equiv \begin{bmatrix} M_{11} & 0 & 0 \\ 0 & M_{22} & 0 \\ 0 & 0 & M_{33} \end{bmatrix} \tag{32}$$

and

$$\left.\begin{aligned} [K_{11}] &= \beta^2 p_{yy}^{-1}[Q_1] + p_{zz}^{-1}[Q_4] \\ [K_{22}] &= \beta^2 p_{xx}^{-1}[Q_2] + p_{zz}^{-1}[Q_5] \\ [K_{33}] &= p_{xx}^{-1}[Q_6] + p_{yy}^{-1}[Q_7] \\ [K_{12}] &= [K_{21}]^\dagger = -p_{zz}^{-1}[Q_8] \\ [K_{23}] &= [K_{32}]^\dagger = -j\beta p_{xx}^{-1}[Q_9] \\ [K_{13}] &= [K_{31}]^\dagger = -j\beta p_{yy}^{-1}[Q_{10}] \end{aligned}\right\} \tag{33}$$

$$\left.\begin{aligned} [M_{11}] &= q_{xx}[Q_1] \\ [M_{22}] &= q_{yy}[Q_2] \\ [M_{33}] &= q_{zz}[Q_3] \end{aligned}\right\} \tag{34}$$

where † denotes the complex conjugate and transverse, and the matrices $[Q_i]$ $(i = 1 \sim 10)$ are given in the Appendix. By applying the Silvester's inequality to (31), the rank of $[K]$ will become equal to that of $[S]$.

Summing the contribution of all elements over the cross section of the waveguide yields

$$F = \sum F^e = \tfrac{1}{2}\left(\{\tilde{V}\}^\dagger [\tilde{K}]\{\tilde{V}\} - \omega^2 \{\tilde{V}\}^\dagger [\tilde{M}]\{\tilde{V}\}\right) \tag{35}$$

where

$$[\tilde{K}] = \sum_e [K] \tag{36}$$

$$[\tilde{M}] = \sum_e [M] \tag{37}$$

where $\{\tilde{V}\}$ is an ordered array of the three-component nodal variables. The matrices $[\tilde{K}]$ and $[\tilde{M}]$ are an adjoint matrix. Hence, the variation of F in (35) gives the follow-

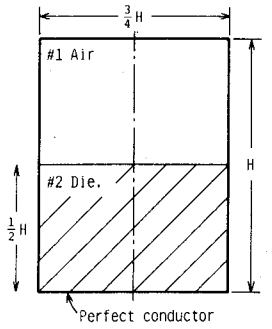

Fig. 3. Cross section of half dielectric-loaded metal waveguide; $\epsilon_1 = \epsilon_0$, $\mu_1 = \mu_0$, $\epsilon_2 = 4\epsilon_0$, $\mu_2 = \mu_0$.

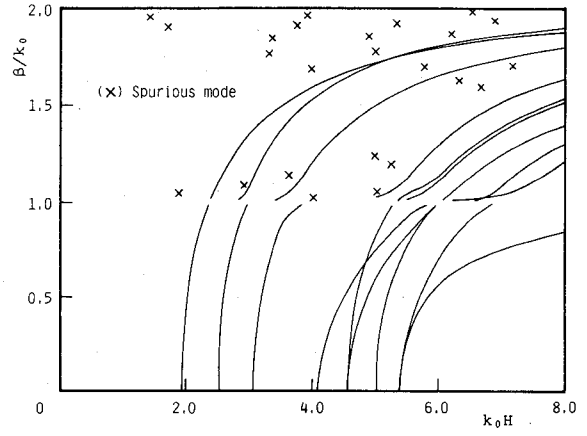

Fig. 4. Dispersion characteristics from two-component finite-element analysis.

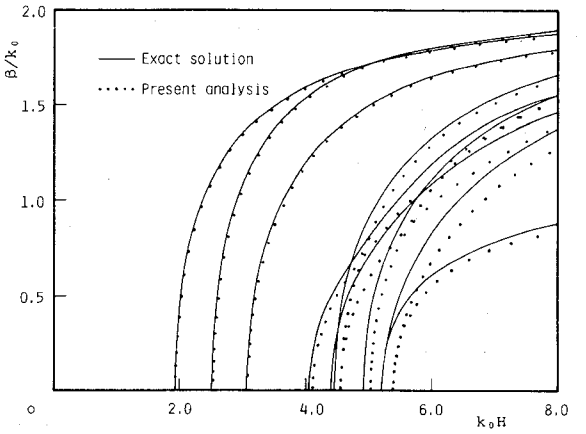

Fig. 5. Comparison of exact solution and present three-component finite-element analysis results.

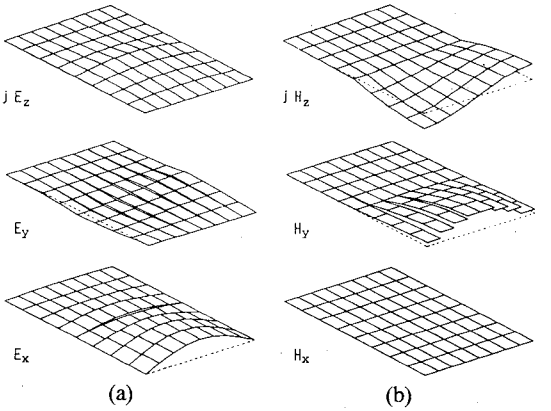

Fig. 6. Plots of field intensity of LSM_{11} mode for (a) E- and (b) H-presentation at $\beta H = 5.0$.

ing algebraic eigenvalue problem:

$$[\tilde{K}]\{\tilde{V}\} - \omega^2[\tilde{M}]\{\tilde{V}\} = 0. \tag{38}$$

The matrix $[\tilde{K}]$ has components proportional to the β^0, β^1, and β^2. The solution of this eigenvalue problem will provide the required results on the angular frequency of various modes on a particular waveguide. From the analogy between the space of the element and the space of the cross section of the waveguide, the rank of $[\tilde{K}]$ is equal to $N_x + N_y$, where N_x and N_y are the number of unknown values of $\{V_x\}$ and $\{V_y\}$, respectively. Therefore, the algebraic system of (38) has N_z zero eigenvalues where N_z is the number of unknown values of $\{V_z\}$. Other field components can be derived from the eigenvector of (38) by (3) or (4).

IV. Examples and Considerations

To demonstrate the excellent quality and the accuracy of the finite-element analysis of the previous section, the solutions for sample problems are given and are compared with the conventional two-component finite-element solutions [2], [3] due to insufficient data of the three-component one [6]. In our program, all the eigenvalues of (38) are obtained.

First, the problem consisting of a rectangular metal waveguide half-filled with dielectric, as shown in Fig. 3, is treated. The propagation modes in this waveguide are classified into LSM, LSE, and TE modes, as is well known. Fig. 4 shows the dispersion characteristics obtained from the two-component finite-element analysis. In Fig. 4, the occurrence of the spurious modes and the difficulties at $\beta/k_0 = 1$ can be found. Fig. 5 shows the dispersion characteristics obtained from the present finite-element analysis for the E-formulation and from the exact solutions. On comparing the results of Fig. 4, the spurious modes have not occurred at all in Fig. 5. And then, it is confirmed from the numerical experiment that the algebraic system of (38) has the implicit zero eigenvalues, of which the number is equal to that of the longitudinal nodal points. All nonzero eigenvalues were found to have one-to-one correspondence to the propagation modes from its field distribution.

Agreement between the finite-element solutions and the exact solutions is excellent. Fig. 6 shows the field intensity configuration of the LSM_{11} mode taken at $\beta H = 5.0$. These field configurations are almost identical with those obtained by the exact solution so that the values of H_x over all cross sections of the waveguide are equal to zero.

Second, a problem consisting of a rectangular metal waveguide with microstrip of finite thickness in the center, as shown in Fig. 7, is treated. This waveguide geometry is given in [2] and the spurious modes were shown to be mixed with physical modes in the solution of the two-component finite-element method. Fig. 8 shows the dispersion characteristics obtained from our method where the spurious modes have not occurred at all and the number of

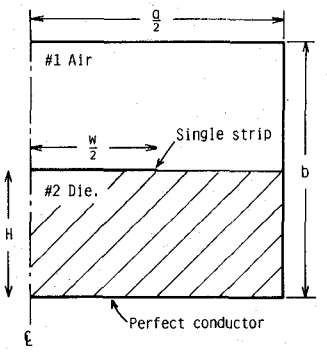

Fig. 7. Half cross section of closed microstrip; $a = 2b = 2W = 4H$.

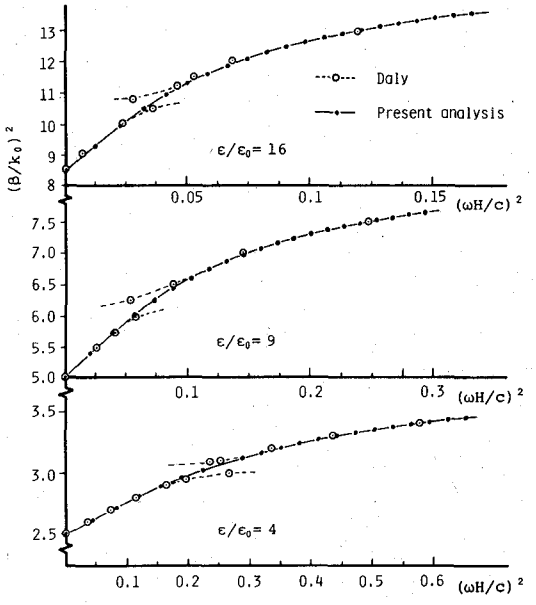

Fig. 8. Comparison of the two-component and present three-component finite-element analysis results.

the zero eigenvalues were confirmed to be equal to that of the longitudinal nodal points, as well.

V. Conclusion

In this paper, the finite-element method for solving the dielectric-loaded waveguide problems was presented in which the nonphysical spurious solutions included in the solution of the two-component finite-element method do not appear. This program has a specific number of zero eigenvalues. The element used in our formulation is restricted to the rectangle, so that the arbitrary cross section of the waveguide must be divided into the small rectangular region.

Future problems in the present finite-element analysis will be the formulation with the triangular element and the treatment of needless zero eigenvalues.

Appendix

The $[Q_i]$ matrices in (33) and (34) are given by

$$[Q_1] = [U_{xx}] \tag{A1}$$

$$[Q_2] = [U_{yy}] \tag{A2}$$

$$[Q_3] = [U_{zz}] \tag{A3}$$

$$[Q_4] = [B_x][U_{00}][B_x]^T \tag{A4}$$

$$[Q_5] = [A_y][U_{00}][A_y]^T \tag{A5}$$

$$[Q_6] = [B_z][U_{yy}][B_z]^T \tag{A6}$$

$$[Q_7] = [A_z][U_{xx}][A_z]^T \tag{A7}$$

$$[Q_8] = [B_x][U_{00}][A_y]^T \tag{A8}$$

$$[Q_9] = [U_{yy}][B_z]^T \tag{A9}$$

$$[Q_{10}] = [U_{xx}][A_z]^T \tag{A10}$$

where

$$[U_{xx}] = \int_{y_1}^{y_2}\int_{x_1}^{x_2}[\varphi_x][\varphi_x]^T dx\,dy = \frac{h_x h_y}{6}\begin{bmatrix}2 & 1\\ 1 & 2\end{bmatrix} \tag{A11}$$

$$[U_{yy}] = \int_{y_1}^{y_2}\int_{x_1}^{x_2}[\varphi_y][\varphi_y]^T dx\,dy = \frac{h_x h_y}{6}\begin{bmatrix}2 & 1\\ 1 & 2\end{bmatrix} \tag{A12}$$

$$[U_{zz}] = \int_{y_1}^{y_2}\int_{x_1}^{x_2}[\varphi_z][\varphi_z]^T dx\,dy = \frac{h_x h_y}{36}\begin{bmatrix}4 & 2 & 2 & 1\\ 2 & 4 & 1 & 2\\ 2 & 1 & 4 & 2\\ 1 & 2 & 2 & 4\end{bmatrix} \tag{A13}$$

$$[U_{00}] = \int_{y_1}^{y_2}\int_{x_1}^{x_2}[\varphi_0][\varphi_0]^T dx\,dy = h_x h_y[1]. \tag{A14}$$

Acknowledgment

The author wishes to thank Prof. H. Kayano for his helpful discussions and advice, and Prof. H. Matsumoto for his helpful advice.

References

[1] P. Silvester, "A general high-order finite-element waveguide analysis program," *IEEE Trans. Microwave Theory Tech.*, vol. MTT-17, pp. 204–210, Apr. 1969.

[2] P. Daly, "Hybrid-mode analysis of microstrip by finite-element methods," *IEEE Trans. Microwave Theory Tech.*, vol. MTT-19, pp. 19–25, Jan. 1971.

[3] M. Ikeuchi, H. Sawaki, and H. Niki, "Analysis of open-type dielectric waveguides by the finite-element iterative method," *IEEE Trans. Microwave Theory Tech.*, vol. MTT-29, pp. 234–239, Mar. 1981.

[4] C. Yeh, S. B. Dong, and W. Oliver, "Arbitrarily shaped inhomogeneous optical fiber or integrated optical waveguide," *J. Appl. Phys.*, vol. 46, pp. 2125–2129, May 1975.

[5] A. Konrad, "Vector variational formulation of electro-magnetic fields in anisotropic media," *IEEE Trans. Microwave Theory Tech.*, vol. MTT-24, pp. 553–559, Sep. 1976.

[6] A. Konrad, "High-order triangular finite elements for electromagnetic waves in anisotropic media," *IEEE Trans. Microwave Theory Tech.*, vol. MTT-25, pp. 353–360, May 1977.

[7] N. Mabaya, P. E. Lagasse, and P. Vandenbulke, "Finite element analysis of optical waveguides," *IEEE Trans. Microwave Theory Tech.*, vol. MTT-29, pp. 600–605, June 1981.

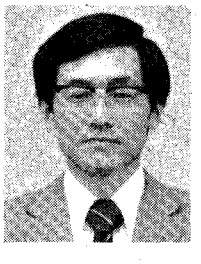

Mitsuo Hano was born in Yamaguchi, Japan, in 1951. He received the B.S. and M.S. degrees in electrical engineering from Yamaguchi University, in 1974 and 1976, respectively.

From 1976 to 1979, he was a member of the Faculty of Science, Yamaguchi University. Since 1979, he has been a member of the electrical engineering faculty at Yamaguchi University. He has been engaged in research of light modulation using the magnetooptic effect and electromagnetic propagation.

Mr. Hano is a member of the Institute of Electrical Engineers of Japan and the Institute of Electronics and Communication Engineers of Japan.